Hindawi Publishing Corporation
Advances in Optical Technologies
Volume 2015, Article ID 236014, 8 pages
http://dx.doi.org/10.1155/2015/236014

Research Article

GaP Homojunction LEDs Fabricated by Dressed-Photon-Phonon-Assisted Annealing

Jun Hyoung Kim,[1] Tadashi Kawazoe,[1,2] and Motoichi Ohtsu[1,2]

[1]*Department of Electrical Engineering and Information Systems, Graduate School of Engineering, The University of Tokyo, 2-11-16 Yayoi, Bunkyo-ku, Tokyo 113-8656, Japan*
[2]*Nanophotonic Research Center, Graduate School of Engineering, The University of Tokyo, 2-11-16 Yayoi, Bunkyo-ku, Tokyo 113-8656, Japan*

Correspondence should be addressed to Jun Hyoung Kim; kimjh@nanophotonics.t.u-tokyo.ac.jp

Received 5 August 2014; Revised 6 November 2014; Accepted 10 November 2014

Academic Editor: Gilles Lerondel

Copyright © 2015 Jun Hyoung Kim et al. This is an open access article distributed under the Creative Commons Attribution License, which permits unrestricted use, distribution, and reproduction in any medium, provided the original work is properly cited.

By using a homojunction-structured GaP single crystal, we generated a photon energy higher than the bandgap energy (2.26 eV). The device was fabricated by performing dressed-photon-phonon- (DPP-) assisted annealing, while applying a forward-bias current, on a p-n homojunction structure formed by implanting a dopant (Zn) into an n-type GaP substrate. The DPP-assisted annealing increased the light emission intensity in an energy band above 2.32 eV by at least 550% compared with that before annealing.

1. Introduction

In recent years, there has been interest in light-emitting diodes (LEDs) as high-efficiency light sources, and research and development has been actively carried out, resulting in remarkable technological progress, particularly in the last ten years. High-efficiency semiconductor light-emitting devices based on InGaN (for light emission in the blue-green band) and AlGaInP (for light emission in the green-red band) have been realized and are now in widespread use. However, there are a number of problems that must be solved. One of those is that a metal-organic vapor phase epitaxy (MOVPE) process, which uses toxic gases, is required for growing the substrates. The environmental load is also high since fine particles that are harmful to the human body could be produced [1]. In addition, finding the optimum conditions for the MOVPE process is not simple, and the growth conditions should be strictly controlled [2–5]. Moreover, this approach has a demerit in terms of material resources, including the need for In, which is a rare earth element.

To overcome the problems mentioned above, in this research we focused on GaP as the material and on dressed-photon-phonon- (DPP-) [6, 7] assisted annealing as the process method. The bandgap energy, E_g, of GaP is 2.26 eV (wavelength, 548 nm). Also, GaP is a low-cost material that can be readily used to grow single crystals with the liquid encapsulated Czochralski (LEC) method, and research into light-emitting devices using GaP has been conducted for a long time, since as early as the 1960s [8, 9]. However, GaP is an indirect transition type semiconductor, and the light-emission efficiency is known to be extremely low since phonon emission and absorption are required for the radiative recombination of electron-hole pairs. A widely known technique for increasing the efficiency is to introduce isoelectronic impurities such as N atoms, and devices based on this approach are commercially available [10]. Isoelectronic impurities capture and localize electrons due to differences in electronegativity with respect to the component atoms of the host crystal. As a result, according to the uncertainty principle, the wave function of the electrons in wavenumber space becomes broader, making radiative recombination possible at yellow and green wavelengths. In addition, GaP LEDs that emit red light by the addition of Zn and O have also been reported [11]. However, the light-emission efficiency is low because of energy loss due to internal relaxation to the isoelectronic impurity levels. Furthermore, only photons

with energies lower than E_g are emitted, since light emission occurs via localized levels in the forbidden band.

On the other hand, if it were possible to effectively utilize the large E_g of GaP, it would be possible to develop a method that overcomes the environment-related problems and technical difficulties mentioned above, as well as to expand the color coverage of GaP LEDs. To this end, in this study we employed a dressed-photon-phonon- (DPP-) assisted annealing method. We have previously used DPPs to develop LEDs based on Si and SiC, which are also indirect transition type semiconductors, like GaP [12–14]. A dressed photon (DP) is a quasiparticle that represents the coupled state of a photon and an electron-hole pair in a nanosize region [7]. Similarly, a DPP is a quasiparticle that represents the coupled state of a DP and multimode coherent phonons in a nanosize region [6, 7]. In other words, by forming an impurity distribution that easily generates an interaction between electron-hole pairs, photons, and phonons inside a crystal, the limitation due to the wavenumber conservation law is relaxed, thus enabling high-efficiency radiative recombination even in an indirect transition type semiconductor [12–14]. The photon energy of this radiative recombination changes by an amount equal to the energies of multimode coherent phonons involved, and therefore, the photon energy of emitted light can be higher than E_g.

In this study, by subjecting a GaP crystal containing a p-n homojunction to DPP-assisted annealing, we obtained strong enhancement of light emission in the 520–540 nm wavelength band.

2. Principles of Light Emission and Processing Using DPPs

In this section, first we explain the principle of light emission using the DPP-assisted process, followed by a discussion of the processing principle. This is because the principle of light emission described below is also used in device processing. The DPP-assisted process [12] brought about as a result of interactions between electron-hole pairs, photons, and phonons in nanosize regions containing impurities is the basic principle of the light emission. During device processing, first, impurities are made to diffuse by changing the energy (via current and photoabsorption) given to the device into heat. In parts that have a nanostructure (impurity distribution) where the DPP-assisted process easily takes place, the energy is converted to light, and therefore, a relative cooling effect occurs [13]. Diffusion of impurities due to heat generation and maintaining the impurity distribution due to the relative cooling are the basic principles of device processing.

The light emission due to the DPP-assisted process can be understood using a model of the DPP levels as shown in Figure 1. Since the wavenumber is supplied from multimode coherent phonons, the DPP dispersion relation is represented by the horizontal green solid line in Figure 1. Since electron-hole pairs and phonons are strongly coupled, the ket vector representing this coupled state is expressed as the direct product ⊗ of the electron state and the phonon state [7]. Here, el and phonon represent electrons and phonons,

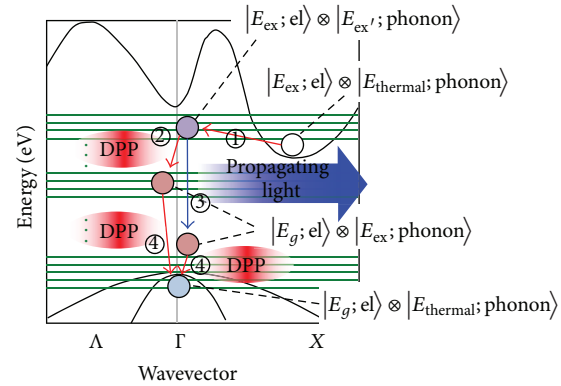

Figure 1: Light emission process via DPPs.

respectively, g represents the ground state, thermal represents thermal equilibrium, and ex and ex′ represent excited states. First, the initial state is formed by injection of carriers from outside. In this initial state, since the electrons are in the excited state, and the phonons are in the thermal equilibrium state determined by the crystal lattice temperature, we have $|E_{ex}; el\rangle \otimes |E_{thermal}; phonon\rangle$. In this state, light emission is obtained via a process in which electrons transition to the ground state $|E_g; el\rangle \otimes |E_{thermal}; phonon\rangle$, that is to say, a process in which they transition to the valence band. This transition occurs via the intermediate states $|E_{ex}; el\rangle \otimes |E_{ex'}; phonon\rangle$ and $|E_g; el\rangle \otimes |E_{ex}; phonon\rangle$. Since transitions to the ground state via these intermediate states are electric-dipole-allowed transitions, not only are DPPs generated (Figure 1, ① → ② → ④), but so is propagating light (Figure 1, ① → ③ → ④). In addition, because of the multimode coherent phonons involved in this process, photon emission with an energy different from E_g is possible. An inverse process to this process, in other words, an absorption process due to DPPs, also exists.

Next, a processing method is described. In an indirect transition type semiconductor, since phonon absorption/emission is necessary during the emission of a photon, the radiative recombination probability is extremely low. However, in the light-emission process via DPPs, since the DP couples with multimode coherent phonons, the radiative recombination probability is high. In other words, an LED can be realized by exciting electrons to the conduction band with current injection and by using the above-described phonon absorption/emission processes. Also, the light emission wavelength of this device depends not on E_g, but on the energy of the DPs generated in the vicinity of the p-n junction. That is to say, emitted light having an energy higher than E_g can be obtained [13, 14]. The problem is that, in the case of a normal semiconductor crystal, the DPP generation probability inside the crystal is low, and it is difficult to bring about transitions via DPP intermediate states. Here, we explain how to form, in a self-organized manner, a nanostructure that readily generates DPPs.

First, p-type impurities are implanted into an n-type substrate to form a p-n junction. Next, while irradiating the p-n junction with laser light, a forward-bias current is made to

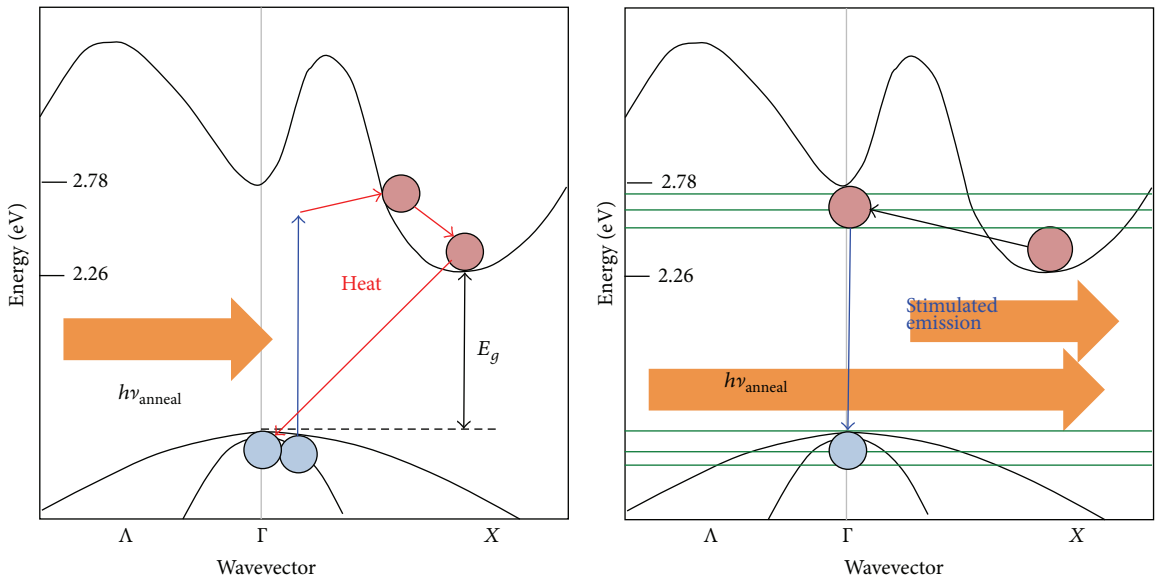

FIGURE 2: Principle of impurity diffusion by DPP-assisted annealing. (a) Heat generation due to light absorption. (b) Relative cooling due to stimulated emission.

flow to perform annealing. This processing method, known as DPP-assisted annealing [7, 12], changes the impurity distribution to a distribution suitable for generating DPPs. In the following, the processing principle is explained by dividing the distribution into a nanoregion that is not suitable for generating DPPs and a nanoregion that is suitable for generating DPPs.

(1) Region Not Suitable for Generating DPPs. If the photon energy of the irradiated laser light, $h\nu_{\text{laser}}$, is larger than E_g, as shown in Figure 2(a), an electron in the valence band absorbs a photon and is excited to the conduction band. This electron immediately emits a phonon due to intraband thermal relaxation and transitions to the bottom of the conduction band. Thermal energy $h\nu_{\text{laser}} - E_g$ is produced via this process. After relaxation, the electron-hole pair cannot undergo radiative recombination because of restrictions due to the wavenumber conservation law and instead undergoes nonradiative relaxation. Since this nonradiative relaxation also generates localized heat, all of the photon energy of the absorbed laser light is converted to thermal energy, causing dopant diffusion to proceed. As a result, Joule heating occurs due to the current, and heat generation occurs due to the nonradiative relaxation caused by the light irradiation.

(2) Region Suitable for Generating DPPs. Since a nonuniform domain boundary formed by the dopant (Zn) is formed inside the crystal by ion implantation at a high acceleration energy, the existence of a region that is suitable for generating DPPs locally can be expected. Let us assume that DPPs are generated around a certain Zn domain. In this case, as shown in Figure 2(b), at the electron-hole pairs, stimulated emission occurs via the DPP levels. As a result, unlike region (1), the locally absorbed energy is converted not only to thermal energy but also to photon energy. Therefore, in the region around this Zn domain, heat generation is suppressed, and the diffusion rate is reduced.

In region (1), random diffusion continuously occurs, whereas in region (2), the diffusion rate is low. These diffusion processes continue until a structure suitable for generating DPPs is achieved. In addition, because the emitted light irradiates the whole device, it is not confined to the light-irradiation region but spreads in a self-organized manner throughout the whole device. When annealing is performed for a sufficiently long time, the concentration of Zn in the entire crystal is expected to take a spatial distribution that is optimal for stimulated emission via the DPP-assisted process. Moreover, since the probabilities of stimulated emission and spontaneous emission are proportional to each other [15], by using such a process, it is possible to realize an LED that emits photons.

3. Device Fabrication

The device fabrication process can be divided into two stages. First, a p-n homojunction structure is fabricated in a GaP single crystal by ion implantation. Then, the impurity distribution is altered by DPP-assisted annealing. The details of these are given below.

In the experiments performed in this study, we used an n-type (dopant: S) GaP single-crystal wafer with a thickness of 500 μm and a diameter of 50 mm, grown by the liquid encapsulated Czochralski (LEC) method. The orientation was (111), and the dopant concentration was 2×10^{17} to $4 \times 10^{17}/\text{cm}^3$ (resistivity, 0.05 Ωcm). This wafer was subjected to ion implantation to implant acceptors (Zn ions) with an implantation energy of 300 keV and a dose of $1.7 \times 10^{14}/\text{cm}^2$ to fabricate a p-n homojunction structure. By

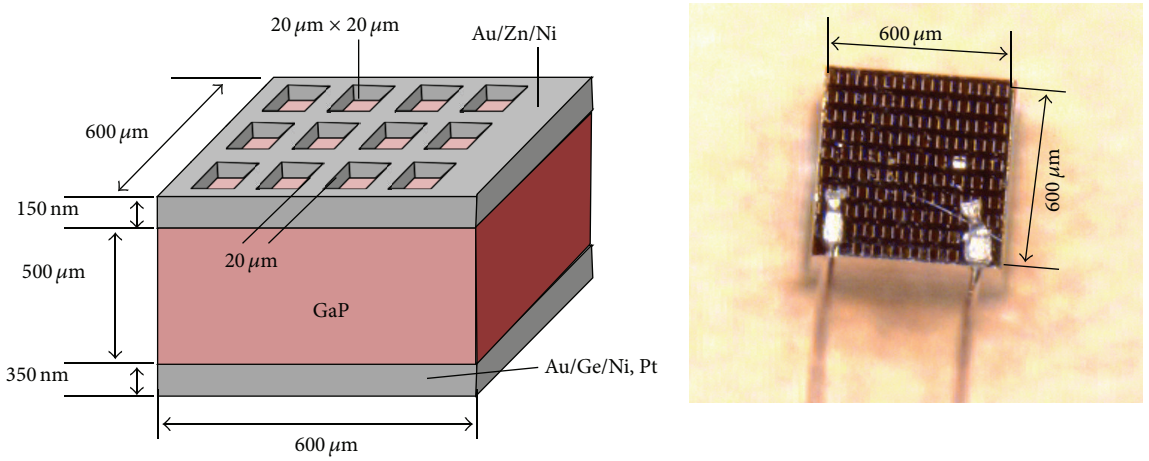

Figure 3: Schematic diagram of device and photograph of completed device.

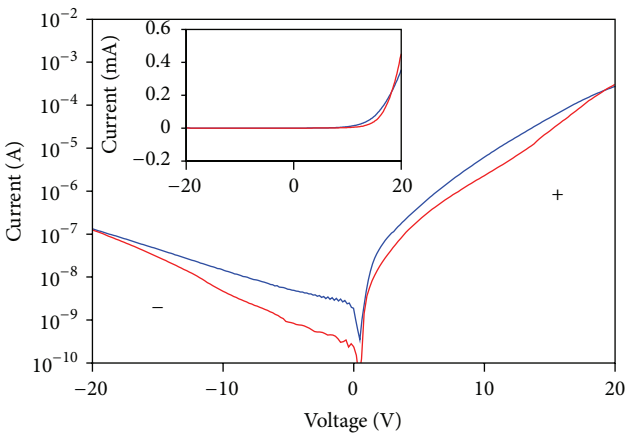

Figure 4: *I-V* characteristic of fabricated device. Red curve: before DPP-assisted annealing. Blue curve: after DPP-assisted annealing.

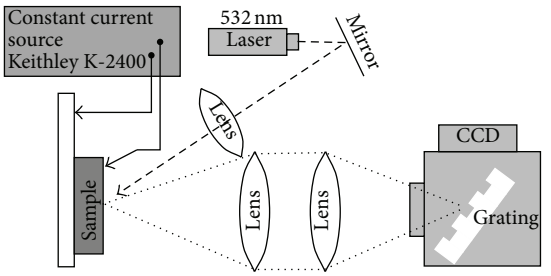

Figure 5: Experimental setup for DPP-assisted annealing and EL spectral measurements.

using such a high acceleration energy, a nonuniform domain boundary was formed, which was expected to form a region suitable for generating DPPs in a localized manner. After ion implantation, the surface was rinsed with HCl to remove excess Zn ions. After this, an Au/Zn/Ni film (150 nm) was deposited on the front surface (p-type side) of the substrate by sputtering and lift-off processing (Figure 3). The electrodes were formed in the shape of a mesh so as to facilitate light irradiation and light emission during DPP-assisted annealing and device driving, respectively. An Au/Ge/Ni film (300 nm) and a Pt film (50 nm) were sequentially deposited on the rear surface (n-type side) to serve as a negative electrode. Then, the wafer was diced into a 600 μm × 600 μm chip and was fixed to a 20 mm × 20 mm × 1.7 mm printed circuit board (PCB) by soldering the negative electrode. Finally, the positive electrode was connected to the PCB by wire bonding. The *I-V* characteristic of the fabricated device is shown in Figure 4 by the red curve. A rectification property was observed, indicating that a p-n junction was formed.

Next, the DPP-assisted annealing will be explained. Figure 5 shows the experimental setup used for DPP-assisted annealing and for measuring the EL spectrum. A K-2400 sourcemeter (Keithley Instruments Inc.) was used as a constant-current source for supplying current during the DPP-assisted annealing and during driving of the device. The emission spectrum of the device was measured using a spectrophotometer and a cooled Si-CCD (Roper Scientific Inc.). To make the device emit light in the green band (wavelengths around 530 nm), a forward-bias current of 30 mA (9.9 A/cm^2) was applied to the device fabricated as described above while irradiating it with 532 nm wavelength (2.32 eV) laser (DPSS CW laser, CNI Inc.) light. The laser power was 0.4 W, and the focal spot diameter on the surface of the device was 0.6 mm (35.4 W/cm^2). During the DPP-assisted annealing, the surface temperature of the device reached 40°C, while the PCB had been cooled to 26°C. As described in Section 2, the spatial distribution of the Zn ions was modified by Joule heat due to the current and by heat generated due to light absorption. The spectrum was measured every 1 hour. The processing was completed when the change in spectral intensity relative to the previous measurement was 1% or less.

4. Device Operation

4.1. Changes in Electroluminescence Spectrum due to DPP-Assisted Annealing. Figure 6(a) shows the results of

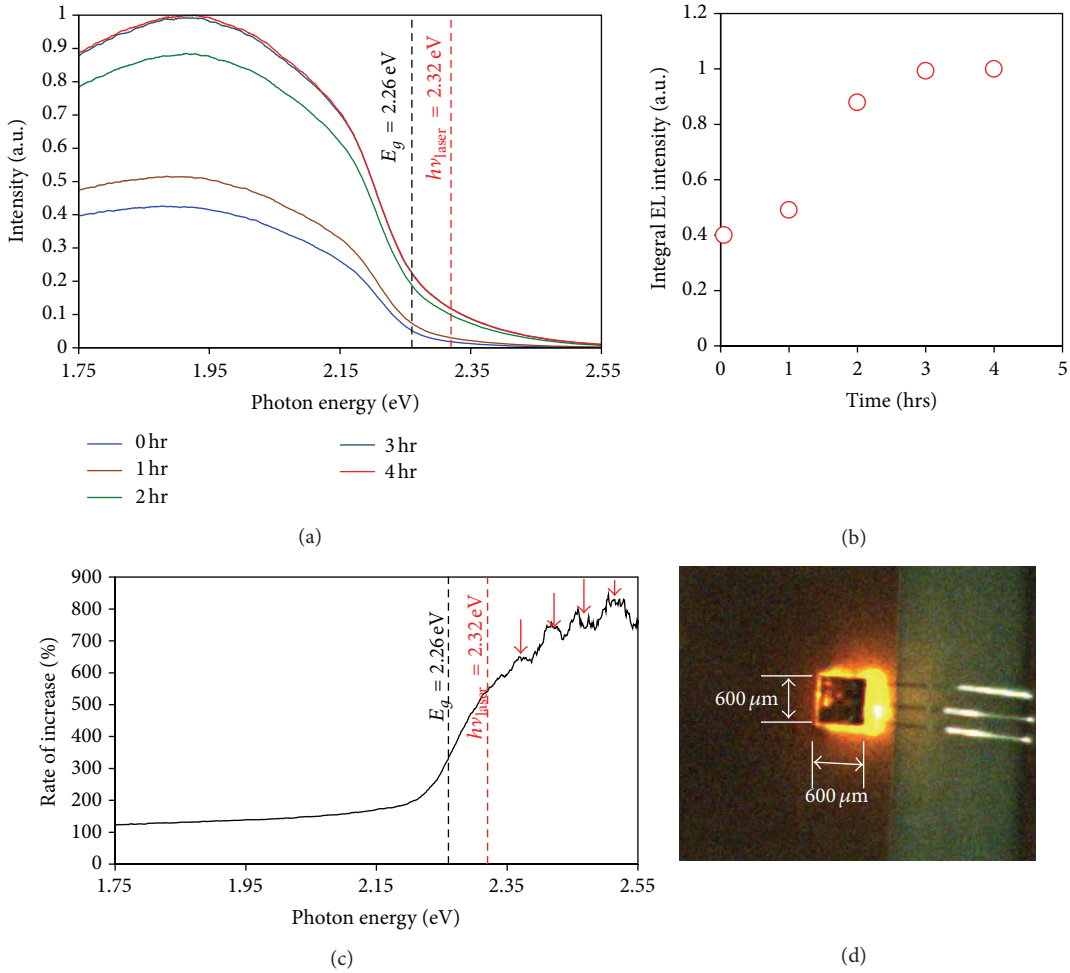

FIGURE 6: Temporal changes in EL spectra during DPP-assisted annealing of GaP LED. (a) Spectra observed during DPP-assisted annealing with a current density of 9.9 A/cm^2 while irradiating device with 532 nm laser light with power of 0.4 W. EL measurements were performed every 1 hour under the same current density conditions (9.9 A/cm^2), but without laser irradiation. (b) Total EL light emission intensity (integral of curve in (a)) versus time. (c) Measured values of R. (d) Light emission from fabricated device.

measuring the EL spectrum of the device during DPP-assisted annealing. The injection current was 30 mA. For reference, the photon energy of the irradiation light (2.32 eV) during DPP-assisted annealing and the bandgap energy of GaP (2.26 eV) are also shown by the vertical red and black dotted lines, respectively. The spectra were measured during an exposure time of 0.25 s, after the laser light irradiation was stopped. This figure shows that the light emission in the range 1.75–2.26 eV has become more intense as the annealing time was increased. Possible explanations for this include light emission from Zn-O pairs formed from Zn atoms and impurity O atoms which occupy the closely spaced Ga site and P site, respectively [16], and light emission originating from radiative recombination of electrons trapped at the donors (S) and free holes [17]. In particular, it has been reported that formation of Zn-O pairs can be explained by diffusion of Zn from the p side to the n side of the p-n junction [18]. In other words, the strong emission intensity in this region as DPP-assisted annealing progressed can be considered evidence that Zn diffusion took place. In addition, light emission was observed from levels above E_g. This was a result of the DPP-assisted process described in Section 2. And the increase in light emission from these high energy levels was a result of the DPP-assisted annealing described also in Section 2.

Figure 6(b) shows the dependence of the total EL light emission intensity (the areas enclosed by the curves and the horizontal axis in Figure 6(a)) on the DPP-assisted annealing time. The light emission intensity saturated after about 3 hours of annealing, reaching an intensity three-times higher than the initial intensity.

Figure 6(c) shows the rate of increase R. It is the normalized emitted light intensity P of the photon energy E after saturation (after 4 hours of DPP-assisted annealing), given by the following expression:

$$R = \frac{P_{4\,\mathrm{hr}}(E) - P_{0\,\mathrm{hr}}(E)}{P_{0\,\mathrm{hr}}(E)}. \quad (1)$$

In this figure, at photon energies below 2.2 eV ($< E_g$), R was 150–250%, whereas at photon energies higher than that of

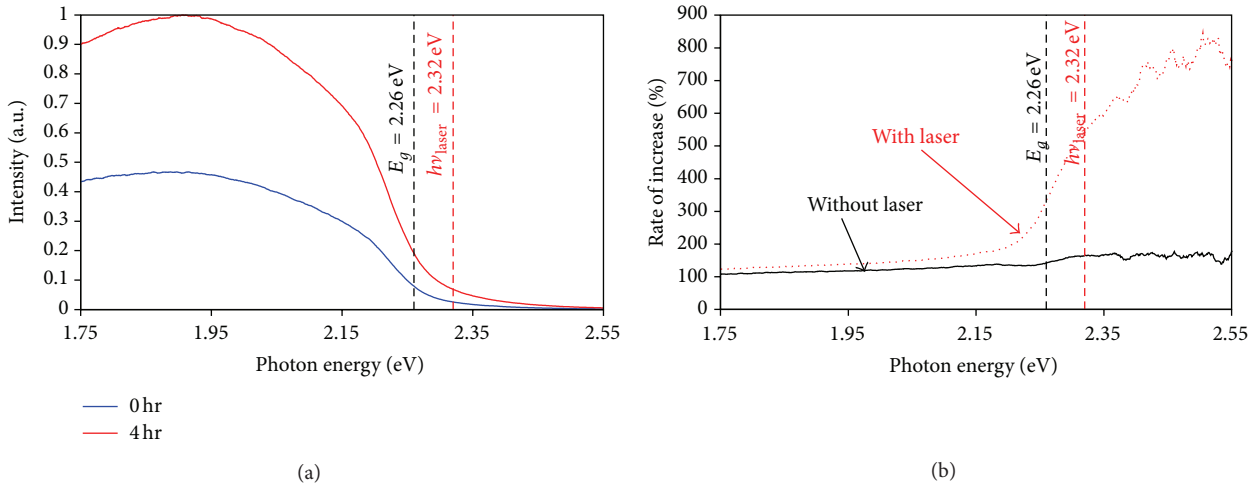

FIGURE 7: Spectrum of device annealed for 4 hours while applying current density of 9.9 A/cm^2 but no laser irradiation. (a) Blue curve shows initial spectrum, and red curve shows spectrum after DPP-assisted annealing for 4 hours. (b) Measured values of R. For comparison with case where annealing was performed without laser irradiation (black curve), the case where annealing was performed with laser irradiation is also shown (Figure 6(c), red curve).

the irradiation laser light ($h\nu_{laser}$), R was 550% or greater. This intensity variation is in agreement with that expected from the discussion in Section 2. In addition, in this figure, periodic peaks (indicated by downward red arrows) are observed at positions away from $h\nu_{laser}$ (=2.32 eV). These peaks were 50 meV apart, which corresponds to the energy of LO phonons in GaP. In other words, phonon sidebands appeared in the emitted light in the high-energy region, as reported in a previous study [19, 20], confirming that the light emission phenomenon was due to a DPP-assisted process via multimode coherent phonons.

Figure 6(d) is a photomicrograph showing light emission from the device. Although the value of R was large at energies higher than the photon energy of the irradiation laser light ($h\nu_{laser}$), the emission component originating from impurities or Zn-O centers [16, 17] was strong, making the emitted light appear orange.

4.2. Effect of Photon Number Density on the DPP-Assisted Annealing. Usually, GaP contains defects or impurities such as oxygen, and these form emission centers. In other words, photons with a wide range of energies are generated inside the crystal during DPP-assisted annealing, and it is thought that stimulated emission is also made possible triggered by these generated photons.

To confirm the effect of this light emission inside the crystal, we performed annealing while causing a current to flow (30 mA), but without laser irradiation. The EL spectrum obtained as a result is shown in Figure 7(a). The black curve in Figure 7(b) is the rate of increase, R, given by (1) (the red curve is a copy of Figure 6(c)). First, the values of this black curve at the low energy side were close to the values of the red curve. However, above E_g, they considerably differed. This feature can be explained as follows. In the 1.7–2.2 eV energy band, the photon number density with the corresponding energy is the same, regardless of whether or not laser irradiation is performed, and therefore, no change occurs in the DPP-assisted process. In addition, the light emission from Zn-O or defects does not change compared with the case where laser irradiation is performed, and therefore, the rate of increase is substantially the same. In the case of the high-energy band, it is thought that there is a difference between progression and suppression of dopant diffusion depending on whether or not laser irradiation is performed. In other words, if monochromatic light of sufficient intensity is made incident, stimulated emission from an energy level corresponding to the photon energy of that monochromatic light becomes more pronounced. Therefore, this demonstrates the effectiveness of DPP-assisted annealing, in terms of the ability to control the photon energy of the light emission from the device by the photon energy, $h\nu_{laser}$, of the irradiation light rather than E_g.

4.3. The Influence of Crystallinity. In general, lattice defects occur in crystals due to impurity doping by ion implantation. In particular, with high-energy ion implantation, there is also a risk of the crystal becoming amorphous. In the present study, light emission was brought about by a DPP-assisted process. However, this process uses high energy during ion implantation, and there is also a study in which a light-emitting device was fabricated using amorphous GaP [21]; therefore, we examined the crystallinity and its influence on light emission.

We used a sample that was preliminarily annealed at 800°C for 30 minutes prior to DPP-assisted annealing, after ion implantation. Figure 8 shows the measured Raman scattering spectra (incident light: 488 nm) of the substrate before ion implantation (blue circles), the substrate after ion implantation (red diamonds), and the substrate after preliminary annealing carried out in a furnace (green triangles). In the spectrum for the substrate before ion implantation, sharp peaks appeared, which indicate the high crystal

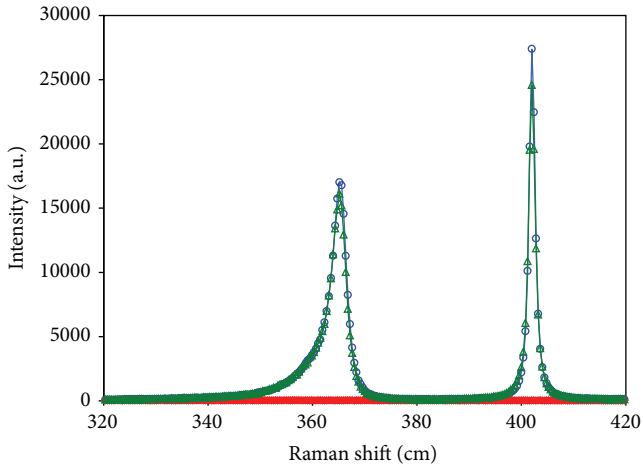

FIGURE 8: Measured Raman scattering spectra. Blue circles: substrate before ion implantation, for comparison. Red diamonds: substrate after ion implantation. Green triangles: substrate subjected to preliminary annealing after ion implantation (800°C, 30 minutes).

quality. However, after ion implantation, these peaks were not observed; therefore, it is considered that the surface changed to an amorphous structure. Also, in the spectrum for the substrate after preliminary annealing, peaks appeared again. To confirm the effect of the amorphous surface on light emission, the substrate whose surface crystallinity was restored by preliminary annealing was formed into a device and was subjected to DPP-assisted annealing under the same conditions. The results are shown in Figure 9. As can be understood from this figure, the same spectral change as shown in Figures 6(a) and 6(c) was observed also in the preannealed sample.

The results shown in Figures 8 and 9 can be explained as follows: by implanting Zn into GaP with a high acceleration energy, namely, 300 keV, the surface of the GaP crystal became amorphous. However, via the DPP-assisted process, the light emission occurs at the domain boundaries formed by the dopant (Zn) inside the crystal and does not rely on the amorphization of the crystal surface. Thus, the same results are obtained regardless of whether or not preliminary annealing is performed to recover the crystallinity.

5. Conclusion

We successfully fabricated a light-emitting device by forming a p-n junction via ion implantation in a bulk GaP crystal, which is an indirect-transition type semiconductor, and by using DPP-assisted annealing. The EL spectrum of the device fabricated by this method was governed by the light used during processing, not by the band structure of the semiconductor. In practice, the light emission from energy levels higher than 2.32 eV was increased by more than 550% (E_g of GaP is 2.26 eV) by using 532 nm (2.32 eV) light irradiation during the DPP-assisted annealing. In contrast, the rate of increase in the energy region below 2.2 eV was limited to 150–250%. By performing experiments with and without

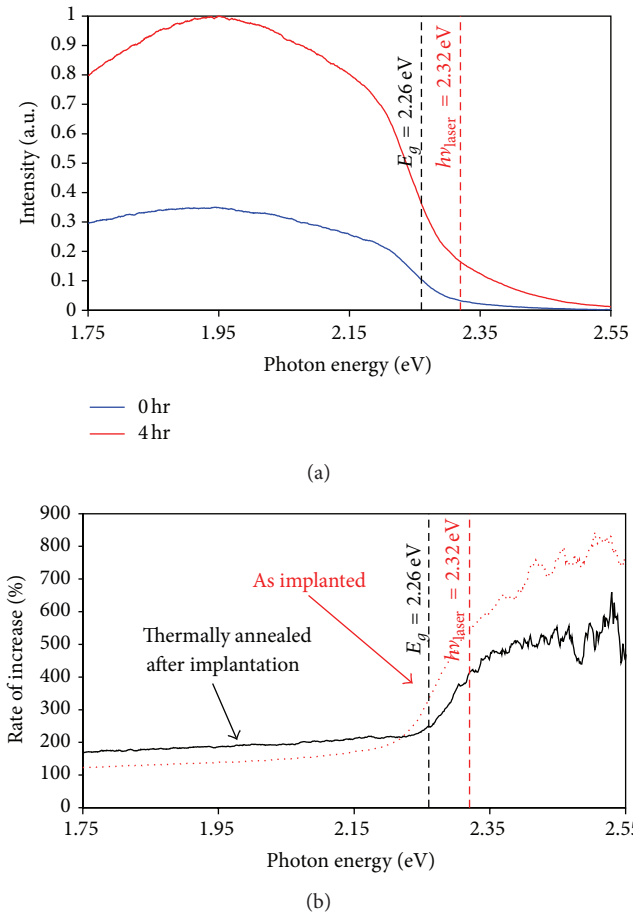

FIGURE 9: Results of DPP-assisted annealing of sample subjected to preliminary annealing after ion implantation. Processing was performed under the same conditions as in Figure 6 (applying current density of 9.9 A/cm^2 while irradiating the device with 532 nm laser light at power of 0.4 W). (a) Comparison of initial spectrum and spectrum obtained at saturation. (b) Rate of increase of EL spectral intensity (black solid curve). Case without preliminary annealing is also shown for comparison (Figure 6(c), red curve).

irradiation light, we also observed a phenomenon whereby the light emission intensity from higher energy levels was increased as a result of the DPP-assisted annealing, thus demonstrating the effectiveness of the DPP-assisted process. In addition, it was also confirmed experimentally that this light was emitted from a single crystal and was not due to amorphization.

Although the light emission from energy levels higher than E_g was remarkably increased, the peak position of the EL spectrum was around 630 nm due to defects and impurity O atoms. Thus, we believe that it will be possible to realize a GaP LED with an emission peak around 530 nm, provided that the crystallinity of the GaP can be improved.

Conflict of Interests

The authors declare that there is no conflict of interests regarding the publication of this paper.

Acknowledgments

The authors received support in Raman spectroscopy from Professor Dr. S. Takagi, Professor Dr. M. Takenaka, and Mr. J.-H. Han of The University of Tokyo. This work was partially supported by a Grant-in-Aid for Scientific Research (B) (no. 24360023) of MEXT and Core-to-Core Program of JSPS.

References

[1] *IARC Monographs on the Evaluation of Carcinogenic Risks to Humans*, vol. 23 of *Some Metals and Metallic Compounds*, World Health Organization, International Agency for Research on Cancer, 1998.

[2] M. Behet, R. Hövel, A. Kohl, A. Mesquida Küsters, B. Opitz, and K. Heime, "MOVPE growth of III–V compounds for optoelectronic and electronic applications," *Microelectronics Journal*, vol. 27, no. 4-5, pp. 297–334, 1996.

[3] P. Fini, X. Wu, E. J. Tarsa et al., "The effect of growth environment on the morphological and extended defect evolution in GaN grown by metalorganic chemical vapor deposition," *Japanese Journal of Applied Physics Part 1*, vol. 37, no. 8, pp. 4460–4466, 1998.

[4] D. D. Koleske, A. E. Wickenden, R. L. Henry, W. J. DeSisto, and R. J. Gorman, "Growth model for GaN with comparison to structural, optical, and electrical properties," *Journal of Applied Physics*, vol. 84, no. 4, pp. 1998–2010, 1998.

[5] P. Gibart, "Metal organic vapour phase epitaxy of GaN and lateral overgrowth," *Reports on Progress in Physics*, vol. 67, no. 5, pp. 667–715, 2004.

[6] Y. Tanaka and K. Kobayashi, "Optical near field dressed by localized and coherent phonons," *Journal of Microscopy*, vol. 229, no. 2, pp. 228–232, 2008.

[7] M. Ohtsu, "Dressed photon technology," *Nanophotonics*, vol. 1, pp. 83–97, 2012.

[8] M. Gershenzon and R. M. Mikulyak, "Light emission from forward biased p-n junctions in gallium phosphide," *Solid State Electronics*, vol. 5, no. 5, pp. 313–329, 1962.

[9] D. G. Thomas, M. Gershenzon, and F. A. Trumbore, "Pair spectra and "edge" emission in gallium phosphide," *Physical Review*, vol. 133, no. 1, pp. A269–A279, 1964.

[10] R. A. Logan, H. G. White, and W. Wiegmann, "Efficient green electroluminescent junctions in GaP," *Solid State Electronics*, vol. 14, no. 1, pp. 55–70, 1971.

[11] J. S. Jayson, R. Z. Bachrach, P. D. Dapkus, and N. E. Schumaker, "Evaluation of the Zn-O complex and oxygen-donor electron-capture cross sections in p-Type GaP: limits on the quantum efficiency of red-emitting (Zn,O)-doped material," *Physical Review B*, vol. 6, no. 6, pp. 2357–2372, 1972.

[12] T. Kawazoe, M. A. Mueed, and M. Ohtsu, "Highly efficient and broadband Si homojunction structured near-infrared light emitting diodes based on the phonon-assisted optical near-field process," *Applied Physics B: Lasers and Optics*, vol. 104, no. 4, pp. 747–754, 2011.

[13] M. A. Tran, T. Kawazoe, and M. Ohtsu, "Fabrication of a bulk silicon p-n homojunction-structured light-emitting diode showing visible electroluminescence at room temperature," *Applied Physics A*, vol. 115, no. 1, pp. 105–111, 2014.

[14] T. Kawazoe and M. Ohtsu, "Bulk crystal SiC blue LED with p-n homojunction structure fabricated by dressed-photon-phonon-assisted annealing," *Applied Physics A*, vol. 115, no. 1, pp. 127–133, 2014.

[15] A. Einstein and P. Ehrenfest, "Zur Quantentheorie des Strahlungsgleichgewichts," *Zeitschrift für Physik*, vol. 19, no. 1, pp. 301–306, 1923.

[16] K. Löhnert and E. Kubalek, "On the degradation of electroluminescence efficiency in gallium phosphide green light emitting diodes," *Physica Status Solidi A*, vol. 80, no. 1, pp. 173–183, 1983.

[17] T. Kawabata and S. Koike, "High-efficiency GaP pure green light-emitting diodes of 555 nm fabricated by new liquid phase epitaxy method," *Applied Physics Letters*, vol. 43, no. 5, pp. 490–491, 1983.

[18] K. Ždánsky, J. Zavadil, D. Nohavica, and S. Kugler, "Degradation of commercial high-brightness GaP:N green light emitting diodes," *Journal of Applied Physics*, vol. 83, no. 12, pp. 7678–7684, 1998.

[19] M. Yamaguchi, T. Kawazoe, and M. Ohtsu, "Evaluating the coupling strength of electron-hole pairs and phonons in a 0.9 μm-wavelength silicon light emitting diode using dressed-photon-phonons," *Applied Physics A*, vol. 115, no. 1, pp. 119–125, 2014.

[20] N. Wada, M. A. Tran, T. Kawazoe, and M. Ohtsu, "Measurement of multimode coherent phonons in nanometric spaces in a homojunction-structured silicon light emitting diode," *Applied Physics A: Materials Science and Processing*, vol. 115, no. 1, pp. 113–118, 2014.

[21] K. Tomioka and S. Adachi, "Structural and photoluminescence properties of porous GaP formed by electrochemical etching," *Journal of Applied Physics*, vol. 98, no. 7, Article ID 073511, 2005.

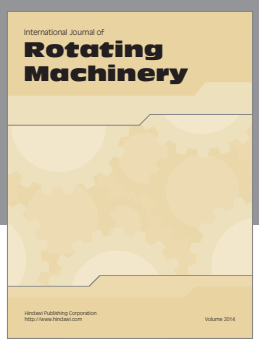

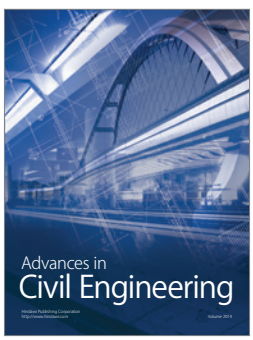

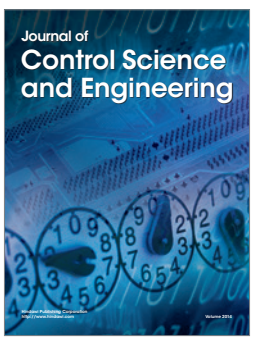

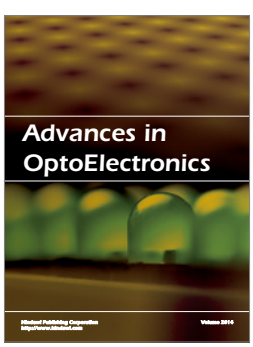

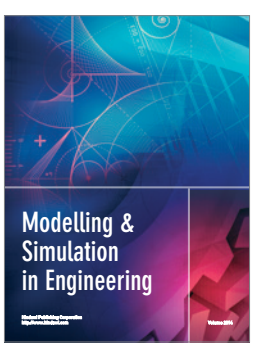

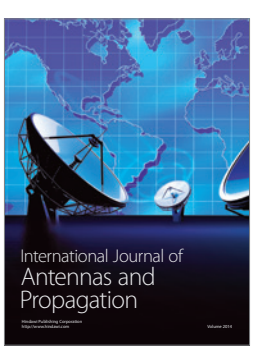

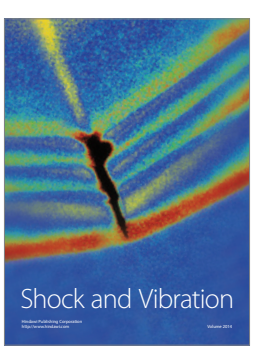

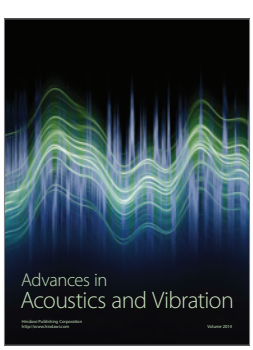

Hindawi

Submit your manuscripts at
http://www.hindawi.com